COMPUTATION OF AIR FLOW AND CONVECTIVE HEAT TRANSFER WITHIN SPACE-CONDITIONED, RECTANGULAR ENCLOSURES.

F. ALAMDARI, G.P. HAMMOND and W.S. MOHAMMAD
Applied Energy Group, School of Mechanical Engineering, Cranfield Institute of Technology, Bedford MK43 OAL, U.K.

Computer simulations are reported of the airflow and convective heat exchange within a warm-air heated, rectangular (three-dimensional) enclosure for which buoyancy effects are significant. Emphasis is placed on meeting the needs of building thermal simulation programs for accurate input data on convective heat transfer. The computations are performed using the 'intermediate-level' convection model of Alamdari and Hammond (1982), and a recently developed high-level 'elliptic' finite-domain flow model. Comparisons are also made with the design recommendations given in some of the established guides. These alternative calculation methods are assessed in terms of the balance they provide between accuracy and economy.

INTRODUCTION

It has been estimated that building services account for about 40-50 per cent of primary energy consumption in industrialised countries (Carroll (1)). The need for efficient use of energy in buildings is therefore obviously important, particularly when viewed against a background of depleting oil and gas reserves. In order to develop realistic methods for the energy-conscious design of buildings, it is necessary to simulate the dynamic thermal response of the system (Clarke (2), Day (3) and Wiltshire (4)). This requires quite sophisticated computational techniques, and has led to an emphasis being placed on modelling the transient performance of the building fabric. In contrast, the air flow and convective heat exchange in and around the structure are simulated using only rough approximations. Indeed, a survey of the new generation of building thermal models for the International Energy Agency (Irving (5)) concluded that their accuracy is presently limited by uncertainties in the input data, particularly for air infiltration and convective heat transfer rates.

In order to obtain improved ways of determining convective heat transfer data appropriate to the needs of building thermal simulation programs, a hierarchy of interacting and interdependent calculation methods have been developed by the authors and their co-workers (see, for example, Alamdari et al (6)). These were originally developed for mechanically-ventilated enclosures, such as warm-air heated rooms or air-conditioned offices, in which the 'forced' convective motion induced by the air supply jet predominates. The calculation methods themselves ranged from 'lower-level' approaches, including analytical solutions and elaborate data correlations for limiting cases, to the development of a 'high-level' flow model that solves a discretized form of the governing partial differential equations for the complex, jet-induced room airflow. Both the higher and lower-level models have been used to develop and verify an 'intermediate-level' computer code (Alamdari and Hammond (7)), which formed the basis for generating input convective heat transfer data for dynamic building models. This code, known as the ROOM-CHT (Room Convective Heat Transfer) program, appears to offer the best prospect of meeting the needs for building thermal simulation in terms of accuracy, economy and user friendliness (6 and 7). The success of this approach led to the development of an analogous intermediate-level computer code for wind-induced, external convection from buildings (6).

The interrelationship between the various calculation methods developed by the authors for computing convection data is illustrated by the schematic diagram shown in Figure 1. The classification scheme adopted for different 'levels' was intended to reflect the potential generality of their range of application, rather than their scientific sophistication (see (6) for a fuller explanation of the choice of terms). The iterative process of developing and verifying intermediate-level methods is represented in Figure 1 by the blocks within the dashed line. Both experimental data, obtained from full and model-scale tests, and the computed results of a higher-level computer code have been used for verification purposes. This was conceived as a feedback process from which ad hoc corrections would be made to the intermediate-level computer

codes where necessary.

In the present contribution a comparative assessment is reported of alternative methods for calculating convective heat exchange within a mechanically-ventilated, rectangular (three-dimensional) enclosure for which buoyancy effects are significant. The calculation methods employed for this 'mixed' convection problem include both the intermediate and higher-level computer codes developed by the authors, together with the design recommendations given in established guides (ASHRAE (8) and CIBSE (9 and 10)). Earlier reports by the authors on their use of a high-level flow model (Alamdari et al (6 and 11)) were limited to cases involving non-buoyant flows in 'two-dimensional' enclosures; restrictions which greatly simplify the computational task. The present evaluation of the various calculation methods is based on the requirements of building thermal simulation programs largely in terms of accuracy and economy.

SPACE-CONDITIONED ENCLOSURE

The warm-air heated room previously used to demonstrate the capabilities of the three-dimensional version of the ROOM-CHT program (7) was adopted for the present study. This represented a corner, ground-floor domestic living room (illustrated in Figure 2), having dimensions 4.30 m length, 2.45 m width and 2.45 m height. Modern practice in the UK would normally utilise warm-air injected through a 'low side-wall register' (12), with supply conditions regulated by a modulating control system (Pimbert (13)). Such a configuration has many potential advantages for 'low energy housing' (7), including good energy efficiency (70-75% over the heating season) and ease of control with rapid response to load changes.

A notional (reference) occupation zone air temperature of $23 \pm 0.5^{o}C$ was adopted for the simulated enclosure, while the surface temperature of the internal walls and ceiling were similarly assumed to remain constant at $21^{o}C$ over the heating season. The two external walls, incorporating single-glazed windows (1.45 m x 1.00 m in the far-wall and 1.80 m x 1.00 m in the side-wall), and the floor were given inside surface temperatures estimated on the basis of best current British practice U-values (14). These temperatures are given in Table 1 as a function of three representative heat loads. The full load condition corresponds to a supply warm-air ventilation rate of 3 air-changes per hour (ACH).

The size of the warm-air supply register was determined by the requirements for full load operation, with face velocities and temperatures within the limits recommended in the British design manual for gas fired systems (12). This suggested a rectangular grille (200 mm x 120 mm, 70% free area) located at the bottom centre of the interior wall, as shown in Figure 2. Such an arrangement gives rise to the formation of a three-dimensional 'wall-jet' (Rajaratnam (15)), which initially spreads out from the terminal device across the floor. Three room air extract grilles are positioned at high-level above the supply register, and these are also illustrated in Figure 2. The supply air conditions would be regulated by the modulating control system, which adjusts a variable-speed fan. This normally operates continuously to give a constant face velocity, whose value depends on the heat load. In contrast, the supply air temperature modulates very slightly about its load-dependent mean value, although this was neglected for the purposes of the present computations. The supply conditions that correspond to the three representative heat loads are

TABLE 1 - Demand-dependent Supply Air Conditions and Surface Temperatures

DEMAND	HEAT LOAD	OUTSIDE AIR TEMPERATURE (^{o}C)	INTERNAL SURFACE TEMPERATURES (^{o}C)		SUPPLY AIR CONDITIONS	
			Exterior Walls and Floor	Windows	Velocity (m/s)	Temperature (^{o}C)
High	Full	-1	16	6	1.50	65
Intermediate	65%	+7	18	11	1.21	55
Low	30%	+15	20	16	0.93	39

again given in Table 1, where the temperatures are those suggested by modern practice (7).

HIGHER-LEVEL MATHEMATICAL MODEL

Background

Air flow and convective heat transfer within an enclosure are governed by the principles of conservation of mass, momentum and thermal energy (or enthalpy). These 'conservation laws' may each be expressed in terms of 'elliptic' partial differential equations, the solution of which provides the basis for a high-level flow model. A discretized form of the governing equations may be obtained by dividing the flow domain into a finite set of small sub-domains, each surrounding a node of the computational grid. The discretized equations are then formulated in such a way that integral conservation requirements are satisfied for individual sub-domains or control volumes. This approach has been called the 'control-volume method' by Patankar (16), and the discretized equations might preferably be distinguished by the prefix 'finite-domain' or 'finite-volume', rather than the term 'finite-difference' commonly employed. The description 'finite-domain equations', suggested by Spalding (17), is adopted here. They are solved in the present higher-level mathematical model by methods similar to those used in the TEACH and CHAMPION family of finite-domain programs developed by Gosman and Pun (18) and Pun and Spalding (19) respectively. Both these codes employ the SIMPLE ('semi-implicit method for pressure linked equations') algorithm of Patankar and Spalding (20), but are restricted to two-dimensional geometries. The authors and their co-workers have therefore used their past experience in applying the CHAMPION code to mechanical ventilation problems (6 and 11) in order to develop a more general computer program capable of simulating three-dimensional flow fields (Alamdari et al (21)). This is called the ESCEAT (Elliptic Equation Solver for Convection and Heat Transfer) code, and was originally employed to compute convective heat transfer in developing, square duct-flow (21). In addition to its ability to handle complex geometries, the program incorporates a number of improvements (described below) in the numerical solution procedure for the finite-domain equations.

Several authors have reported high-level flow model computations for three-dimensional mechanically-ventilated enclosures with both buoyant and non-buoyant conditions. Hjertager and Magnussen (22) developed a finite-domain computer code based on the SIMPLE algorithm (20) which they used to predict the flow and thermal field in a room with a high side-wall register and adjacent ceiling extracts. Buoyancy effects were introduced by way of heated panels in the floor and far wall, together with a cooled air supply. Closure of the finite-domain equations for this turbulent flow was obtained using the popular 'two-equation', 'energy-dissipation' turbulence model (Launder and Spalding (23)), an extended form of which has been adopted for the present study. The authors' comparisons with experimental data (22) displayed good agreement for the isothermal case, although not for the buoyant one. They appear to have made an allowance for buoyancy effects in the mean-flow equations, but not in the turbulence model ones. It is therefore not surprising that their computations were less satisfactory for strongly buoyant flows. A subsequent study by Sakamoto and Matsuo (24) using an early finite-difference technique examined the isothermal flow in a rectangular room with a square, ceiling-mounted supply air 'diffuser' and a low side-wall extract. They employed two different turbulence closure approximations: the standard energy-dissipation model (23) and a more advanced 'large eddy simulation' approach. Comparison with their own experimental mesurements (24) displayed fairly good agreement for the mean-flow field, although not for some of the turbulence properties. Discrepancies were equally apparent with both turbulence closure assumptions, and the authors therefore recommended the use of the simpler energy-dissipation model on grounds of computational economy. Gosman et al (25) used this model, together with a three-dimensional version of the TEACH program, to compute the isothermal flow field in a rectangular enclosure having a square high side-wall register. They report comparisons with mean-flow data that they obtained using laser-Doppler anemometry in a small-scale test rig. This facility had an essentially 'through-flow' geometry with a large low-level slot extract in the far wall. The jet supply conditions were specified using wall-jet empirical data (15) to prescribe the flow properties within an inlet cell. This obviated the need for the very finely-spaced grid that would have been required if computations included the region near the inlet register. The practice also helps to ensure good agreement with the experimental mean-flow measurements. None of the authors of these previous studies (22, 24 and 25) utilised their computer codes to calculate surface heat exchange, as is done in the present one. Each study involved a rectangular cell with no provision for the realistic simulation of window effects. The influence of window downdraught on room air flow is usually very significant, even with forced convective heating or cooling systems.

Mathematical Framework

The governing time-averaged, elliptic equations for the turbulent flow and thermal field may be written in a common form, using tensor notation (25):

$$\frac{\partial}{\partial x_j}(\rho u_j \phi) = \frac{\partial}{\partial x_j}\left[\Gamma_\phi \frac{\partial \phi}{\partial x_j}\right] + S_\phi \quad \text{.....(1)}$$

CONVECTION DIFFUSION SOURCES OR SINKS

Here u_j (u_1, u_2, u_3) are the time-averaged (mean) velocity components in the coordinate directions x_j(x_1,x_2,x_3 : see Figure 2), ϕ are any of the dependent variables [u_j , H ($\equiv C_p T$), k or ε], Γ_ϕ are the effective (laminar plus turbulent) diffusion coefficients for these ϕ's , S_ϕ are the sources or sinks for each ϕ , and ρ is the fluid density. Closure of the equation set was achieved in the present study by using an extended version of the energy-dissipation turbulence model (23) in order to compute an isotropic 'eddy' viscosity, or turbulent exchange coefficient for momentum (μ_t). This requires the simultaneous solution of two additional transport equations for the turbulence kinetic energy (k) and its dissipation rate (ε). The extension to the standard k - ε model (23) involved the inclusion of buoyancy generation or source terms (G_B) in these equations, using a modified form to that suggested by Rodi (26). Mathematical expressions for the diffusion coefficient and source terms for each variable are given in Table 2 and its accompanying notes. The thermal energy equation was modelled using the effective Prandtl number (σ_{eff}) approach (Hammond (27)), and the fluid properties for air were assigned values corresponding to those at the reference temperature.

In order to bridge the steep dependent variable gradients close to the room surface, the ESCEAT code employs so-called 'wall-functions' (23). These are simply based on the well-known bilogarithmic behaviour of the mean velocity and temperature near solid walls. The resultant velocity in planes parallel and close to any surface may therefore be obtained from the following expression, which utilises conventional near-wall scaling (23 and 27):

$$v_p^+ = \frac{1}{\kappa} \ell n\ (E\ n_p^+) \quad \text{.....(2)}$$

where n_p is the normal distance from the surface to a nearby point, and the log-law constants were given values previously adopted by one of the present authors (27) : κ = 0.41 and E = 8.4. The corresponding expression for the temperature has the form:

$$T_p^+ = \sigma_t\ (v_p^+ + P_J) \quad \text{.....(3)}$$

with P_J = -1.55 for air-flows. The value for the turbulence energy near the wall (k_p) was calculated from the transport equation for k (see Table 2), but with its diffusion to the wall set equal to zero : $\partial k / \partial n = 0$. In addition, the generation and dissipation terms are usually modified to be consistent with the known results for near-wall flows (19 and 23):

$$G_k = \tau_w \frac{\partial v}{\partial n}\ ,\ G_B = 0 \quad \text{and} \quad \varepsilon = \frac{C_\mu\ f_\varepsilon\ \rho k_p^{\ 2}}{\tau_w} \frac{\partial v}{\partial n} \quad \text{.....(4)}$$

where τ_w is the wall shear stress, and f_ε = 1. However, when computations were undertaken using this practice, the heat balance on the warm-air heated room resulted in load-dependent temperatures in the occupation zone that were unrealistically high ($t_R \simeq 32\text{-}34^oC$). This zone was defined in the manner suggested by Nevins and Miller (28), and its average temperature was adopted as the reference value (T_R). In order to reduce this temperature it was found necessary to set f_ε = 0.05, following the procedure formerly employed (23) for backward-facing surfaces in gas turbine film-cooling simulations. The authors of the latter study argued that in recirculating flows the convected fluid is largely responsible for determining the rate of turbulence energy dissipation to the wall; a situation which is also likely to prevail in the present case. The use of this practice here resulted in occupation zone temperatures of 22.5, 23.0 and 23.5°C for the low, intermediate and high heat loads respectively. In both sets of computations, the near-wall value for the energy dissipation rate itself (ε_p) was determined from the usual presumption (19 and 23) that the turbulence length scale is proportional to the distance from the wall; implying $\varepsilon_p \propto k_p^{3/2}/n_p$.

Numerical Solution Procedure

The generalised set of differential equations, Equation (1), may be formally integrated over each cell volume V_p of the computational grid to yield:

$$\sum_{\text{all b}} \left[\int_{A_b} \left(\rho u_j \phi - \Gamma_\phi \frac{\partial \phi}{\partial x_j} \right)_b \right] dA_b - \int_{V_p} S_\phi\ dV = 0 \quad \text{.....(5)}$$

Table 2 - Diffusion Coefficients and Source Terms in the Governing Elliptic Equations

CONSERVED PROPERTY	ϕ	Γ_ϕ	S_ϕ
Mass (continuity)	1	0	0
Direction - i momentum	u_i	μ_{eff}	$-\frac{\partial P}{\partial x_i} + \frac{\partial}{\partial x_j}\left(\mu_{eff}\frac{\partial u_j}{\partial x_i}\right) - \rho g_i \beta\theta$
Thermal energy (enthalpy)	H	$\frac{\mu_{eff}}{\sigma_{eff}}$	0
Turbulence Kinetic energy	k	$\frac{\mu_{eff}}{\sigma_k}$	$G_K + G_B - \rho\varepsilon$
Turbulence energy dissipation	ε	$\frac{\mu_{eff}}{\sigma_\varepsilon}$	$\frac{\varepsilon}{k}\left(C_1(G_K + G_B) - C_2\,\rho\varepsilon\right)$

Notes

1. $\mu_{eff} \equiv \mu + \mu_t = \mu + \frac{C_\mu \rho k^2}{\varepsilon}$; $\sigma_{eff} \equiv \mu_{eff} \Big/ \left(\frac{\mu}{\sigma} + \frac{\mu_t}{\sigma_t}\right)$

2. $G_K = \mu_t \frac{\partial u_i}{\partial x_j}\left(\frac{\partial u_i}{\partial x_j} + \frac{\partial u_j}{\partial x_i}\right)$; $G_B = g_i \beta \frac{\mu_t}{\sigma_t}\frac{\partial \theta}{\partial x_i}$

3. $\theta \equiv T - T_R$, where T_R is the reference temperature

4. Values for the turbulence model 'constants':

   $C_\mu = 0.09$, $C_1 = 1.43$, $C_2 = 1.92$, $\sigma_t = 0.85$, $\sigma_k = 1.00$ and $\sigma_\varepsilon = 1.30$

where the velocities and coordinate directions are normal to the cell boundary (b) considered, and A_b is the area of this boundary. Here the first term summation is performed over all six boundaries of the cell, while the associated integrals represent the total transport (J_b) by convection and diffusion across each boundary. These integrals may be written in the following, finite-domain form (16):

$$J_b = C_b\phi_p + \left\{ D_b\,\alpha(|Pe_b|) + [\![0, -C_b]\!] \right\}(\phi_p - \phi_b) \qquad \ldots\ldots(6)$$

where C_b ($\equiv \rho u_b A_b$) is the convection term, D_b ($\equiv \Gamma_b A_b/\delta x_{np}$), is the diffusion term, Pe_b ($= C_b/D_b$) is the 'cell Peclet number', and $\alpha(|Pe_b|)$ is a weighting function, while the symbol $[\![a,b]\!]$ denotes the greater of a and b. In the ESCEAT code the weighting function is evaluated using a 'power-law' differencing scheme (16) $\alpha(|Pe_b|) = [\![0, (1-0.1|Pe_b|)^5]\!]$. This scheme yields improved accuracy over some of the older approaches, such as the upwind (19) or hybrid (18 and 25) schemes. The source term integral in Equation (5) is evaluated using a linearised expression ($S_p + S'_p\phi_p$) in order to enhance numerical stability (16, 18 and 19). This is particularly important when S_ϕ is a function of the variable ϕ itself, such as in the case of the k and ε equations (see Table 2). Thus, integration of Equation (5) in the above manner leads to finite-domain equations for each of the dependent variables in the form:

$$(a_p - S'_p)\,\phi_p = \sum_n a_n\phi_n + S_p \qquad \ldots\ldots(7)$$

where the coefficients $a_n = D_n\alpha(|Pe_n|) + [\![0, \pm C_n]\!]$, and $a_p = \sum_n a_n$. The velocity components are calculated in the ESCEAT code at staggered locations mid-way between adjacent grid nodes (20).

This practice has the advantage of ensuring that the velocities are directly available for calculating the convective fluxes of the scalar variables, as well as lying between the location of the static pressures that drive them. However, it necessitates minor changes to the coefficient expressions, as outlined in Mohammad's thesis (29).

The set of algebraic finite-domain equations represented by Equation (7) are solved in the ESCEAT code in an iterative, 'line-by-line' manner (16 and 19), using a tri-diagonal matrix algorithm (19 and 20). Here the velocities and pressures are calculated via the SIMPLEC algorithm, recently proposed by Van Doormaal and Raithby (30). This is a variant of the SIMPLE algorithm (20) which is more consistent, and consequently induces a faster rate of convergence. The latter is also enhanced by the adoption of a plane-by-plane 'block-correction' procedure applied by sweeping the flow domain in the x_3 - direction (see Figure 2). These block adjustments were based on the requirements for overall mass and momentum conservation. The computational grid employed for the present simulation of the warm-air heated room utilised a 17x17x15, non-uniform nodal network, whose fineness can be judged by the velocity vector diagrams presented in Figure 3. In the previous two-dimensional high-level flow model computations by the authors (6 and 11) a jet inlet cell was utilised, over which the variation of the dependent variables was prescribed. This reduced the need for a finely-spaced grid near the supply register. However, it is difficult to prescribe the near-register flow and thermal field in a strongly buoyant situation, such as the present one. Consequently, a jet inlet cell has not been employed in the current study, for which about 700 iterations were required to obtain a converged solution. The latter was assumed to have been obtained when the finite-domain equations were satisfied to within 0.5% or less of the inlet mass flow, or the heat supplied in the case of the H-equation. Further details of the ESCEAT code, including the measures taken to ensure grid-independent solutions in the present case, will be reported elsewhere (29).

INTERMEDIATE-LEVEL MATHEMATICAL MODEL

The ROOM-CHT program (7) prescribes the flow and thermal field within mechanically-ventilated enclosures using the known characteristics of turbulent wall-jets (15). These jets are the normal means of air distribution in buildings with forced convective heating or cooling systems. They are assumed to spread out from their supply register and sequentially flow over the room surfaces. The code was developed in both two- and three-dimensional versions (7), to facilitate the simulation of enclosures with supply apertures in the form of either linear slots or rectangular grilles. The mean-flow properties for the three-dimensional version used here are calculated from wall-jet empirical data (15). These are then employed to determine the corresponding local heat transfer distribution over the room surfaces, using the 'optimum log-law' devised by Hammond (31) on the basis of wall-jet profile analysis. The convection coefficient h_c $[\equiv q_w/(T_R - T_w)]$ may locally fall below that for buoyancy-driven motion at the corresponding temperature difference. Under such conditions the latest version of the code uses the improved correlating equations for buoyancy-driven convection recently developed by Alamdari and Hammond (32). These are rather elaborate, continuous functions that cover the full range of laminar, transitional and turbulent airflows.

The equations which constitute the ROOM-CHT program are generally explicit, algebraic ones, except for the heat transfer log-law which is implicit and is solved using the Newton-Raphson iterative method. Nevertheless, the estimation of initial values for the flow field parameters from experimental data (15) enables a convergent solution to be obtained very rapidly; typically in about three iterations. The computational grid normally employs around 10 uniformly-spaced calculation points per metre length of surface. The surface-averaged heat transfer coefficients are obtained by numerical integration of the local distributions. Fuller details of the mathematical content of the ROOM-CHT program are given in the previous papers of the authors (6,7,11,31 and 32).

A limitation of all intermediate-level models (6) is that they have a restricted range of application, and need to be used in conjunction with a broad flow classification scheme (see Figure 1). In the present case, the ROOM-CHT program is only valid for air distribution systems in which the supply air jet is emitted near, and runs parallel to, one of the room surfaces. Nevertheless, this is not a serious weakness as building thermal modellers are well used to working with problem-specific input data. A potentially more serious restriction for such models is that, because they are 'generalisations' of lower-level ones for simple shear flows, they cannot deal rigorously with the consequences of flow interactions. Wall-jets within space-conditioned enclosures, for example, are influenced by jet-impingement against backward-facing walls, and by 'secondary flows' or longitudinal vortices along streamwise corners (6 and 11). Rather ironically, it has recently been found (11) that in the former situation the ROOM-CHT program was better able to compute surface heat exchange than a high-level flow model. This was because the ability of models of the latter type to determine surface heat transfer is hampered by limitations in the present generation of turbulence model wall functions, despite the fact that they can more accurately simulate complex flow patterns. The flow interaction which is

of central concern to the present study is that induced by buoyancy effects. These are modelled explicitly in the ESCEAT code by incorporating buoyancy source terms in the x_2- direction momentum, k and ϵ transport equations (Equation (1) and Table 2). In contrast, the ROOM-CHT program is unable to take account of such effects in any rigorous manner. It is essentially a non-buoyant model, which only allows for buoyancy-driven convection when the corresponding heat transfer coefficient is greater than the prevailing forced convection value, and then only in an approximate way (6 and 7). Consequently, differences between the computed local heat transfer distributions reported in the following section are primarily due to this cause.

COMPUTATIONS

Flow Field

Velocity vector diagrams illustrating the flow pattern within the warm-air heated room under full heat load conditions are shown in Figure 3. These plots were obtained using the ESCEAT code, and display vectors in the $x_2 - x_3$ plane at three positions which coincide with those of the air extract grilles. Here the tail of each velocity vector indicates the location of a node in the finite-domain computational grid. It is therefore evident that these nodes were concentrated close to the room surfaces, as well as to the jet inlet. This arrangement was adopted in order to provide more nodes in those regions where there are steep dependent variable gradients. The computed flow pattern can be seen to be strongly influenced by buoyancy effects, due to the high temperature of the supply air and the counteracting cold downdraught induced by the windows. In particular, the downdraught from the window in the right wall (viewed from the supply register) clearly damps the rigorous buoyant flow in the rest of the enclosure. The pattern in the latter region is characterised by two recirculating flow regions: one dominated by the buoyant supply jet and the other by the cold downdraught from the window in the far-wall. The ability of high-level flow models to simulate complex flows, such as this, are their major achievement in comparison with intermediate-level ones. A velocity vector diagram produced by the ROOM-CHT program would simply show a wall-jet circulating around the enclosure, with no obvious influence of buoyancy. This would not be adequate for determining, for example, the thermal comfort conditions in the occupation zone, which would require a high-level simulation.

Convective Heat Transfer Coefficients

The local distribution for the convection coefficients corresponding to the above flow pattern are displayed as 'carpet' plots in Figure 4. Here the computed variation over each of the room surfaces according to both the ESCEAT and ROOM-CHT programs are presented. The almost flat distributions given by the intermediate-level code for the near- and side-walls arises because the surface coefficient there is computed from elaborate correlating equations for buoyancy-driven convection (32). These yield a constant, surface-averaged coefficient whenever the local forced convection coefficient would otherwise fall below this value. In contrast, the peculiar peak in the distribution predicted by the high-level flow model near the supply register (see Figure 4 (d)) is simply a consequence of air entrainment into the jet, which causes locally high velocities and heat transfer rates around this rectangular aperture. It is again clear from these carpet plots that the ESCEAT code is better able to simulate the influence of buoyancy, here on heat transfer. However, although there are obviously differences emanating from the neglect of buoyancy effects in the ROOM-CHT program, these are not significant from the point of view of building thermal simulation.

Dynamic building thermal models normally employ heat transfer coefficients that are surface-averaged over each building element (6 and 7): ceilings, floors, roofs, walls and windows. Such values are presented for the warm-air heated room and all three representative heat loads in Table 3, together with those recommended as 'typical' values in the section of the UK CIBSE Guide which deals with the thermal response of buildings (10). In contrast to the latter recommendations, the heat transfer section of the Guide (9) provides an approximate correction factor to buoyancy-driven convection data when the air velocity over a particular surface is non-zero. This practice is not, in reality, very helpful as the designer generally has no means of determining this velocity *a priori* (7). Nevertheless, the authors in a previous study estimated the surface-averaged air velocities for the present enclosure, using the ROOM-CHT program in order to determine the convection coefficient in this way. These turned out to be significantly lower than those given in Table 3 (see (7)), and only slightly above those that would apply for purely buoyancy-driven convection (32). The corresponding room-averaged coefficient at full heat load was found to be 2.3 $W\,m^{-2}K^{-1}$. This value may be compared with those computed by the ESCEAT code and the ROOM-CHT program, which were found to be some 60% higher and are given in Table 4. The ASHRAE Handbook in the USA (8) appears to ignore the possibility of forced convective heating or cooling, and employs only buoyancy-driven coefficients to obtain fabric 'U-values'. These would again fall well below the values given in Tables 3 and 4. It is apparent from these tables that the convection data obtained with the high-level and intermediate-level computer codes are in generally good agreement for this particular room/heating

TABLE 3 - Internal Surface-averaged Convection Coefficients (h_c, $Wm^{-2}K^{-1}$)

SURFACE ELEMENT	HEAT LOAD/ DEMAND	CALCULATION METHOD		
		ESCEAT	ROOM-CHT	CIBSE (10)
FLOOR	Full	2.4	6.4	1.5
	Intermediate	1.9	6.1	1.5
	Low	1.7	5.1	1.5
FAR-WALL	Full	2.4	3.5	3.0
	Intermediate	2.1	3.2	3.0
	Low	1.6	2.8	3.0
FAR-WINDOW	Full	2.2	3.5	3.0
	Intermediate	2.0	3.1	3.0
	Low	1.5	2.6	3.0
CEILING	Full	6.9	3.9	4.3
	Intermediate	6.9	3.4	4.3
	Low	4.1	2.2	4.3
NEAR-WALL	Full	2.2	2.4	3.0
	Intermediate	2.3	2.2	3.0
	Low	1.5	1.6	3.0
RIGHT-WALL	Full	3.6	2.5	3.0
	Intermediate	3.4	2.2	3.0
	Low	2.5	1.8	3.0
RIGHT-WINDOW	Full	2.2	3.5	3.0
	Intermediate	2.0	3.1	3.0
	Low	1.5	2.6	3.0
LEFT-WALL	Full	3.3	1.8	3.0
	Intermediate	3.2	1.7	3.0
	Low	2.2	1.5	3.0

system configuration, except for the ceiling and floor. The latter surfaces are the ones that are most directly affected by the upward trajectory of the buoyant jet on leaving the supply register (see Figures 3(b), 4(a) and 4(c)). It is rather surprising that the typical values suggested in the CIBSE Guide Part A5 (10) yields coefficients for this case that are of comparable accuracy to those of the ROOM-CHT program. This seems to be merely a fortuitous occurrence, which has arisen because these values are, in reality, significantly higher than those that would prevail with the buoyancy-driven convection that they purport to represent. They cannot be relied upon to yield accurate data for other mechanically-ventilated enclosures.

Economy

The present simulations using the ESCEAT code required about 5 hours of central processor unit (CPU) time per run (heat load) on a DEC VAX 11/785 computer. This compares with a CPU time of only one minute using the ROOM-CHT program. These dramatic savings in running time achieved by the intermediate-level model, are accompanied by a need for only one third of the computer storage

TABLE 4 - Notional Room-averaged Convection Coefficients (h_c, $Wm^{-2}K^{-1}$)

HEAT LOAD/ DEMAND	CALCULATION METHOD		
	ESCEAT	ROOM-CHT	CIBSE (10)
Full	3.7	3.5	3.0
Intermediate	3.5	3.2	3.0
Low	2.4	2.6	3.0

requirement. Thus, high-level flow models require computational resources that are of the same order as building thermal models themselves. It would not therefore be a realistic approach to directly couple such computer codes together (6). Any gain in terms of accuracy, over lower- and intermediate-level methods, would be far outweighed by the extra resources consumed.

CONCLUDING REMARKS

Several lessons may be drawn from the computations of air flow and convective heat transfer within a warm-air heated room presented here. It is evident that high-level flow models, such as the ESCEAT finite-domain program, are capable of simulating the complex flow patterns generated within the enclosure. Accurate prediction of the flow and thermal field would be needed in order to determine, for example, the occupation zone thermal comfort conditions. However, the far greater computer resources that they require, compared to simpler calculation methods, would prohibit their direct use in providing input heat transfer data for building thermal simulation programs. In contrast, the authors and their co-workers previously demonstrated (6) that their intermediate-level convection models can be fairly readily incorporated into these programs as subroutines. A better use of high-level flow models in the context of heat transfer would therefore be for the development and verification of intermediate-level calculation methods. The simple guidelines for specifying convection coefficients that are contained in Part A5 of the CIBSE Guide (10) were shown to give surprisingly good agreement with the ESCEAT code surface-averaged values. Nevertheless, it has been argued here that this was only a fortuitous occurrence, that does not justify the use of these guidelines for enclosures employing other mechanical-ventilation systems. This is particularly so in warm-air heated rooms where the supply air is discharged vertically over an adjacent window, giving rise to high convection rates from the latter element. Likewise, air-conditioned offices using linear diffusers would also lead to locally high heat transfer rates over the surface near the supply aperture that could not be accounted for using the CIBSE guidelines. Intermediate-level calculation methods could be readily adapted to handle these situations.

ACKNOWLEDGEMENTS

The work reported here was partially supported by a UK Science and Engineering Research Council research grant GR/C/2419.0, and forms part of the Council's specially promoted programme on 'Energy in Buildings'. One of the authors (WSM) is grateful to the Military Technical College, Baghdad, Iraq, for the sponsorship that enabled him to contribute to this study. All the authors appreciate the care with which Mrs. A. Stalley prepared the camera-ready typescript and Mrs. K. O'Connell traced the figures.

The authors' names appear alphabetically.

SYMBOLS USED

A_b = area of finite-domain cell boundary [Equation (5)]

a = coefficients in finite-domain equations [Equation (7)]

C_b, C_n = convection term in finite-domain equations [Equations (6) and (7)]

C_p = fluid specific heat at constant pressure (J $Kg^{-1}K^{-1}$)

C_μ, C_1, C_2 = 'constants' in the k-ε turbulence model [Table 2]

D_b, D_n = diffusion term in finite-domain equations [Equations (6) and (7)]

E = wall function log-law 'integration' constant [Equation (2)]

f_ε = near-wall k-equation dissipation term parameter [Equation (4)]

G_B = buoyancy generation term in the k-equation [Table 2]

G_K = shear generation term in the k-equation [Table 2]

g_i = gravitational vector ($g_1 = g_3 = 0$, $g_2 = -9.81$ m s^{-2})

h_c = convective heat transfer coefficient (W $m^{-2}K^{-1}$)

H = enthalpy (J Kg^{-1})

J_b = total transport by convection and diffusion across finite-domain cell boundaries [Equation (6)]

k = turbulence kinetic energy (m^2s^{-2})

n = normal distance from a surface or wall (m)

n^+ = $u_\tau n/v$

Pe_b, Pe_n = finite-domain cell Peclet number [Equation (6) and (7)]

P_J = Jayatillaka's P-parameter [Equation (3)]

$\dot{q}$ = convective heat flux (W m^{-2})
Sp, Sp' = coefficients in linearised finite-domain source expression [Equation (7)]
S_ϕ = sources or sinks for the variable ϕ [Equation (1)]
t = temperature (C)
T = absolute temperature (K)
T^+ = ρ Cp u_τ $(T - T_W)/q_W$
u_i = velocity components in the x_i -direction (m s^{-1})
u_τ = 'wall shear' velocity ($\equiv \sqrt{\tau_W/\rho}$, m s^{-1})
v = resultant velocity in planes parallel and close to a surface or wall (m s^{-1})
v^+ = v/u_τ
W = x_l — direction width of the enclosure (m)
x_i = coordinate directions (m)

Greek Symbols

β = coefficient of cubic expansion ($\simeq T_R^{-1}$ for air, K^{-1})
Γ_ϕ = effective diffusion coefficients for each variable ϕ [Equation (1)]
ε = turbulence energy dissipation rate (m^2 s^{-3})
θ = $T - T_R$ (K)
κ = von Karman's constant [Equation (2)]
μ = dynamic viscosity (kg $m^{-1}s^{-1}$)
ν = kinematic viscosity (m^2s^{-1})
ρ = fluid density (Kg m^{-3})
σ = Prandtl number
τ = shear stress (N m^{-2})
ϕ = any dependent variable [Equation (1)]

Subscripts

eff = effective (laminar plus turbulent)
n = neighbouring node in finite-domain grid
p = central node in finite-domain grid
R = reference (or occupation zone) conditions
t = turbulent
w = wall (or surface) conditions

REFERENCES

1. Carroll, D., 1982, "Energy Consumption and Conservation in Buildings : An International Comparison", Proc. 3rd Int. Symp. "Energy Conservation in the Built Environment", 1A, 190, Dublin, Ireland.

2. Clarke, J.A., 1985, "Energy Simulation in Building Design", Adam Hilger, Bristol, England.

3. Day, B., 1982, Computer-aided Design 14, 49.

4. Wiltshire, T.J., 1983, Sun at Work in Britain, No.16, 19.

5. Irving, S.J., 1982, Computer-aided Design 14, 33.

6. Alamdari, F., Hammond, G.P., and Melo, C., 1984, "'Appropriate' Calculation Methods for Convective Heat Transfer from Building Surfaces", Proc. First UK National Heat Transfer Conf., 2, 1201, Leeds, England.

7. Alamdari, F., and Hammond, G.P., 1982, "Time-dependent Convective Heat Transfer in Warm-air Heated Rooms", Proc. 3rd Int. Symp. "Energy Conservation in the Built Environment", 4, 209, Dublin, Ireland.

8. ASHRAE, 1981, "Handbook of Fundamentals", ASHRAE, New York, USA.

9. CIBSE Guide, C3 : "Heat Transfer", 1976, CIBSE, London, England.

10. CIBSE Guide, A5 : "Thermal Response of Buildings", 1979, CIBSE, London, England.

11. Alamdari, F., Hammond, G.P., and Montazerin, N., 1986, "Heat/Mass Transfer Beneath a Two-dimensional Wall-jet Deflected by a Normal, Flat-plate Obstruction", Proc. 8th Int. Heat Transfer Conf., San Francisco, USA, (In Press).

12. Warm Air Group - SBGI, 1976, "Gas Fired Warm Air Heating : British System Design Manual", Ernest Benn, London, England.

13. Pimbert, S.L., 1978, Gas Marketing 22(8), 6.

14. The Electricity Council, 1981, "The Medallion Award Specification", EC 4155.

15. Rajaratnam, N., 1976, "Turbulent Jets", Elsevier, Amsterdam, Netherlands.

16. Patankar, S.V., 1981, Numerical Heat Transfer 4, 409.

17. Spalding, D.B., 1981, Mathematics and Computers in Simulation 23, 267.

18. Gosman, A.D., and Pun, W.M., 1974, "Calculation of Recirculating Flows", Imperial College (London Univ.) Mech. Eng. Dept. Report HTS/74/2 (Second Edition).

19. Pun W.M., and Spalding, D.B., 1976, "A General Computer Program for Two-dimensional Elliptic Flows", Imperial College (London Univ.) Mech. Eng. Dept. Report HTS/76/2 (Amended 1977).

20. Patankar, S.V., and Spalding, D.B., 1972, Int. J. Heat Transfer 15, 1787.

21. Alamdari, F., Hammond, G.P., Macaskill, C., and Mohammad, W.S., 1986, "Thermal Boundary Condition Effects on Turbulent Heat Transfer in Developing, Square Duct-flow", Paper in preparation.

22. Hjertager, B.H., and Magnussen, B.F., 1977, "Numerical Prediction of Three-dimensional Turbulent Buoyant Flow in a Ventilated Room", Spalding, D.B., and Afgan, N. (Editors), "Heat Transfer and Turbulent Buoyant Convection", 2, 429, Hemisphere, Washington, USA.

23. Launder, B.E., and Spalding, D.B., 1974, Comput. Methods Appl. Mech. Eng. 3, 269.

24. Sakamoto, Y., and Matsuo, Y., 1980, Appl. Math. Modelling 4, 67.

25. Gosman, A.D., Nielsen, P.V., Restivo, A., and Whitelaw, J.H., 1980, ASME J. Fluids Eng. 102, 316.

26. Rodi, W., 1980, "Turbulence Models and Their Application in Hydraulics", International Association for Hydraulics Research, Delft.

27. Hammond, G.P., 1985, AIAA Journal 23, 1668.

28. Nevins, R.G. and Miller, P.L. 1972, ASHRAE Trans. 78, 235 (Paper No. 2258)

29 Mohammad, W.S., 1986, PhD. Thesis, Cranfield Institute of Technology, (In preparation).

30. Van Doormaal, J.P., and Raithby, G.D., 1984, Numerical Heat Transfer 7, 147.

31. Hammond, G.P., 1982, "Profile Analysis of Heat/Mass Transfer Across the Plane Wall-jet", Proc. 7th Inst. Heat Transfer Conf., 3, 349, Munich, Germany (FRG).

32. Alamdari, F., and Hammond, G.P., 1983, BSER & T 4, 106.

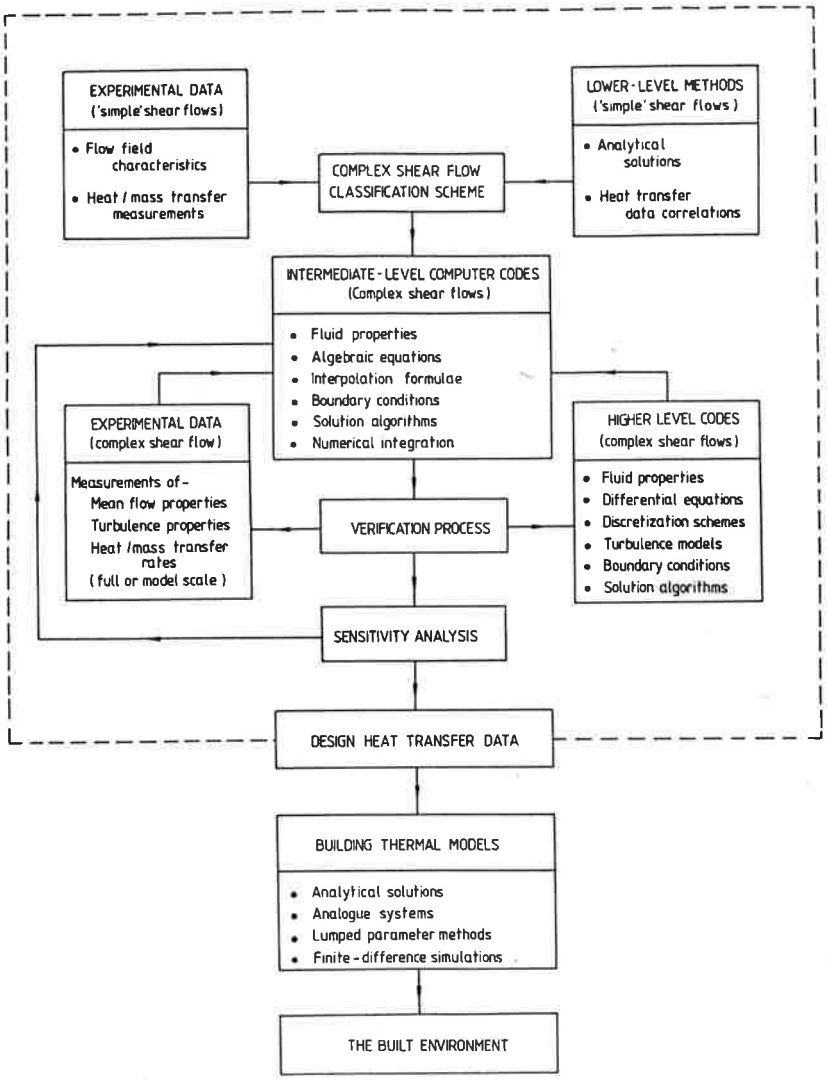

Figure 1. Interrelationship Between the Various Calculation Methods for Building Convective Heat Transfer (6)

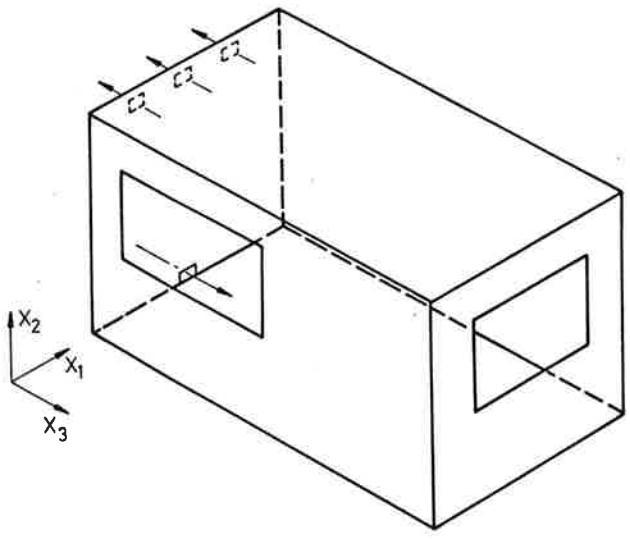

Figure 2. Schematic Diagram of Warm-air Heated Room with 'Low Side-wall Register' (7)

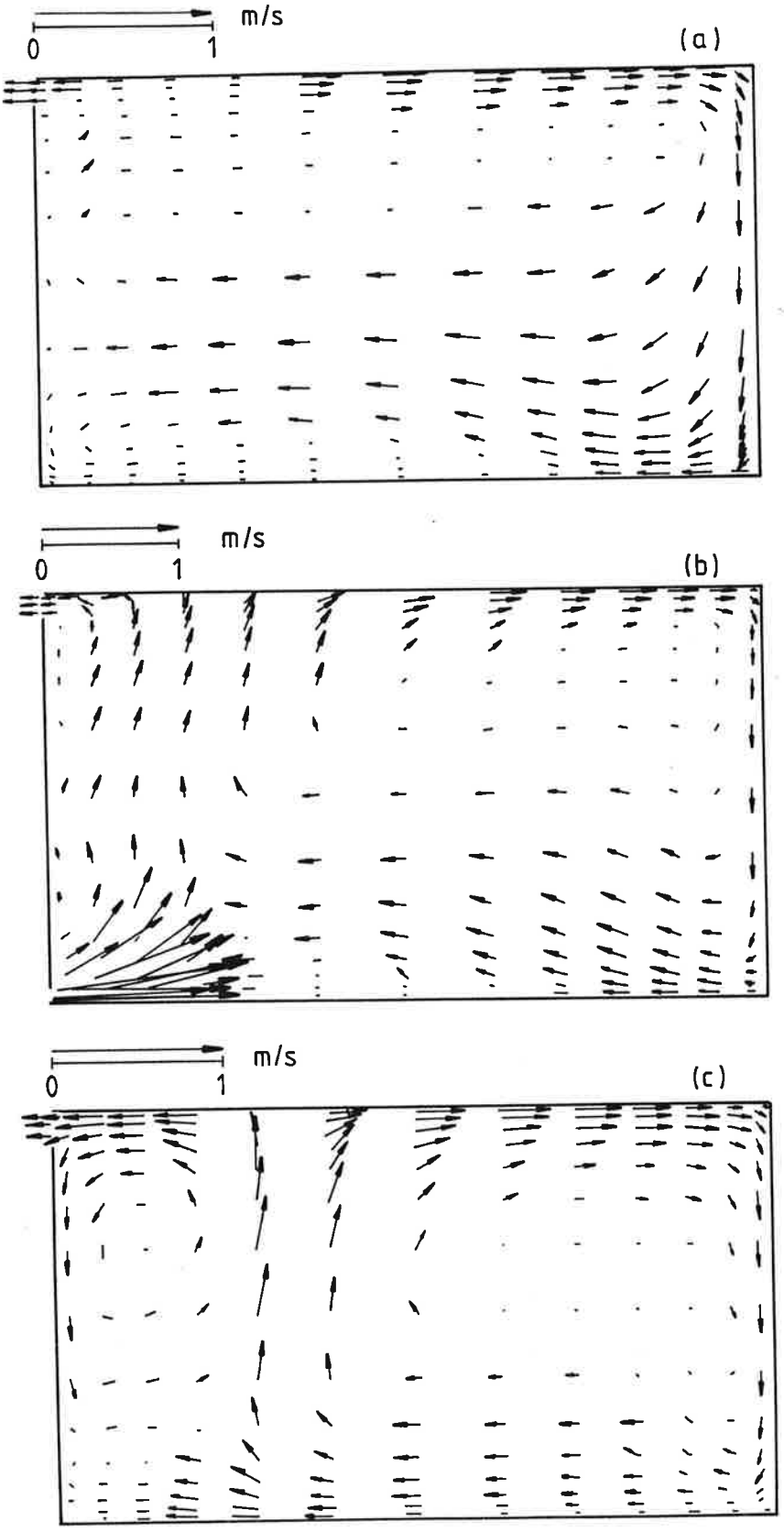

Figure 3. Flow Field Velocity Vectors (Computer Using the ESCEAT Code) : (a) $x_1/W = 0.25$, (b) $x_1/W = 0.50$, (c) $x_1/W = 0.75$ [Note scale change.]

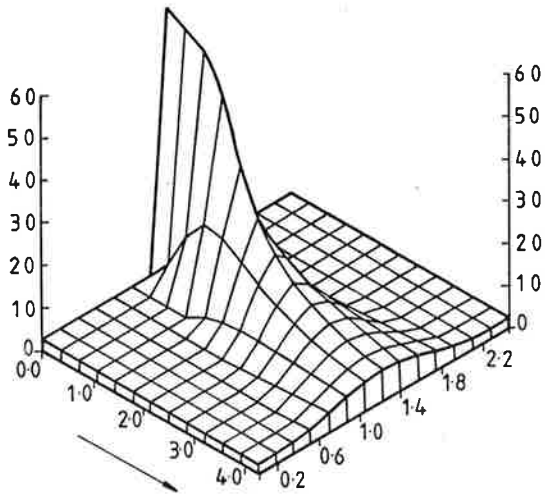

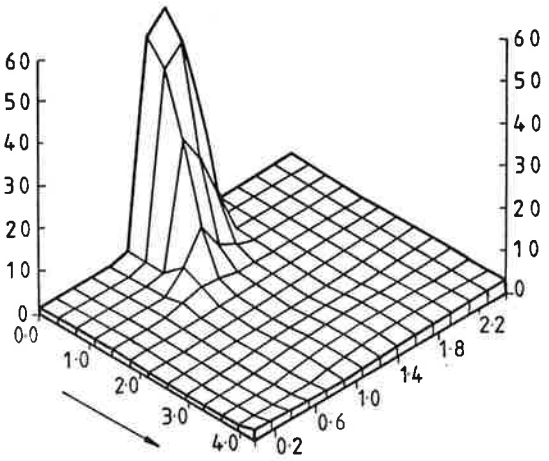

(a) Floor

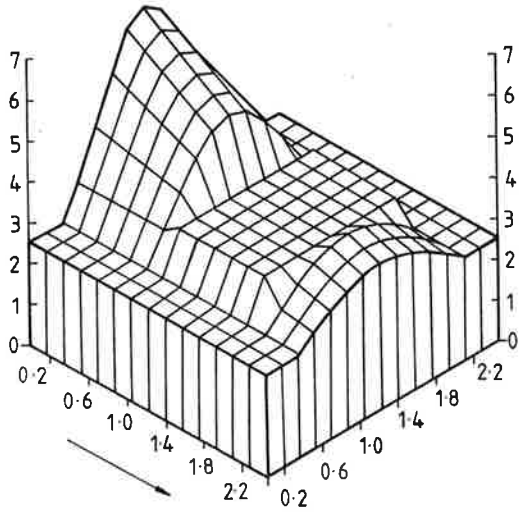

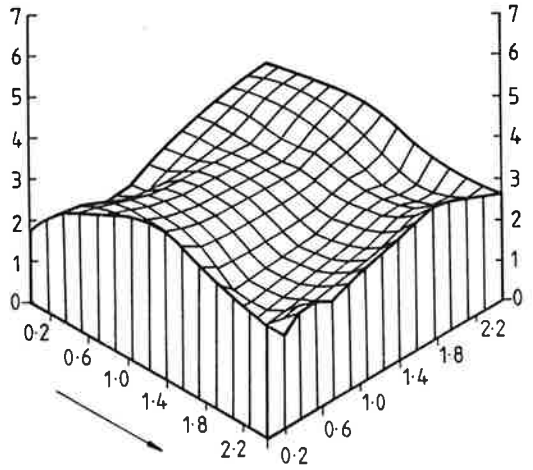

(b) Far-wall and window

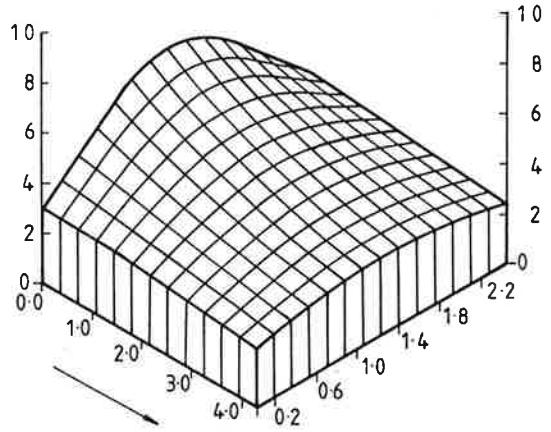

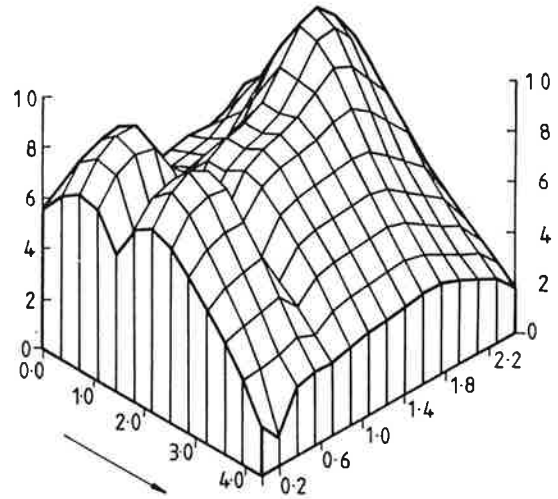

(c) Ceiling

Figure 4. Room Surface Convective Heat Transfer Distributions (h_c, W $m^{-2}K^{-1}$)
: LHS - ROOM-CHT Program, RHS-ESCEAT Computer Code.

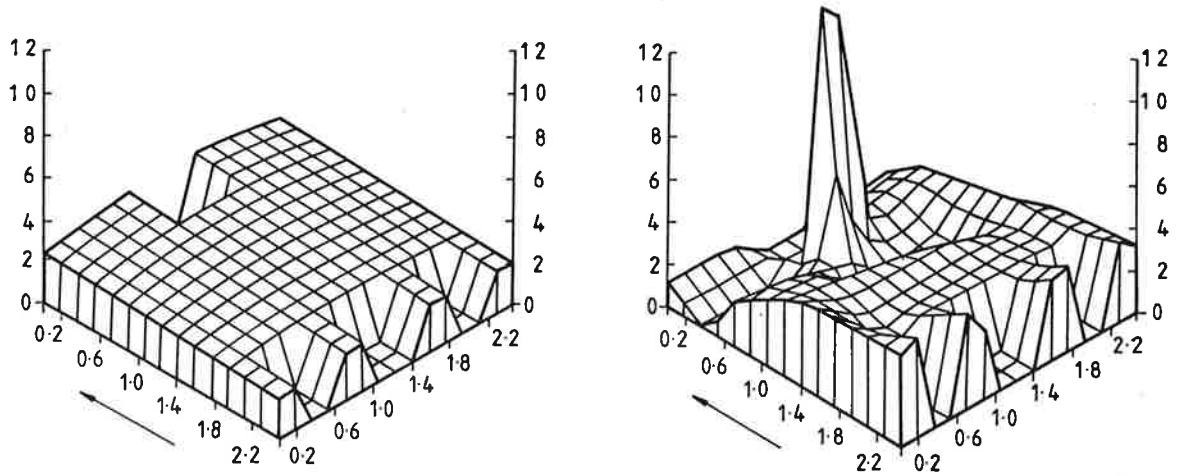

(d) Near-wall

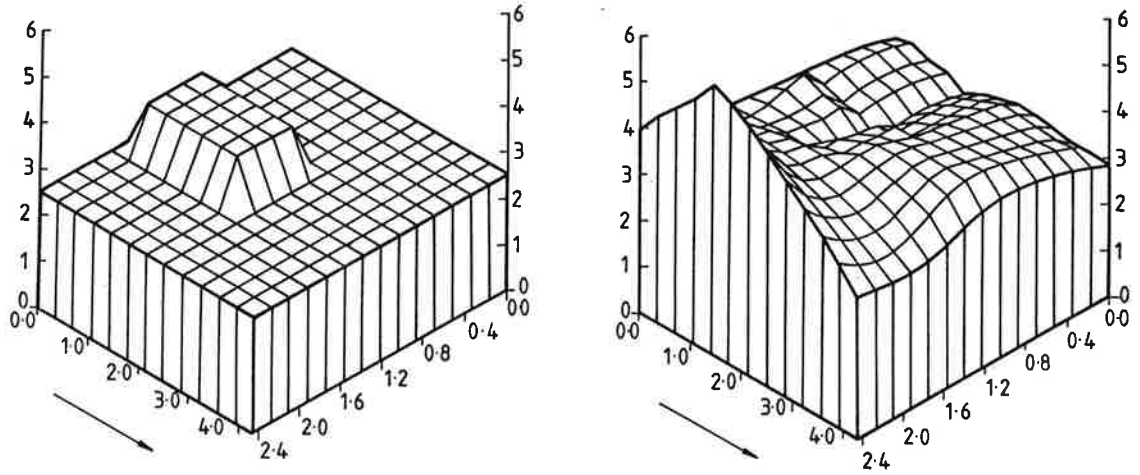

(e) Right-wall and window

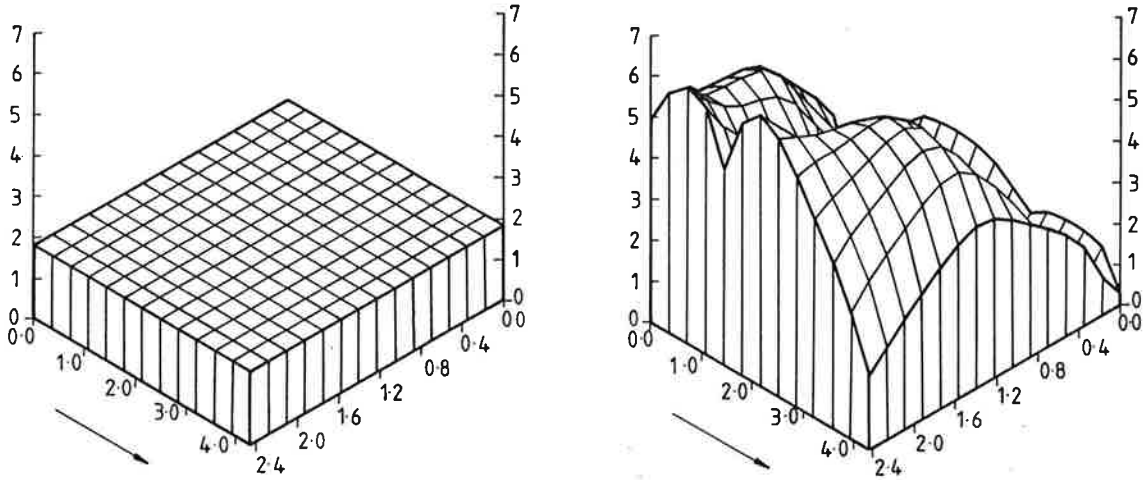

(f) Left-wall

Figure 4 continued...